

# Gluon Polarization in $e^+e^- \rightarrow t\bar{t}G$

S. Groote, J.G. Körner and J.A. Leyva<sup>1</sup>

Institut für Physik, Johannes-Gutenberg-Universität,  
Staudinger Weg 7, D-55099 Mainz, Germany

## Abstract

We calculate the linear and circular polarization of gluons radiated off top quarks produced in  $e^+e^-$ -annihilations. For typical top pair production energies at the Next-Linear-Collider (NLC) the degree of linear polarization remains close to its soft gluon value of 100% over almost the whole energy spectrum of the gluon. The circular polarization is largest for maximal gluon energies where the linear polarization is smallest. The massive quark results are compared with the corresponding results for the massless quark case.

---

<sup>1</sup>On leave of absence from CIF, Bogotá, Colombia

# 1 Introduction

The polarization of gluons in  $e^+e^-$ -annihilation [1, 2], in deep inelastic scattering [3] and in quarkonium decays [1, 4] has been studied in a series of papers dating back to the early 80's. Several proposals have been made to measure the polarization of the gluon among which is the proposal to measure angular correlation effects in the splitting process of a polarized gluon into a pair of gluons or quarks [5].

The earlier calculations of the gluon's polarization in  $e^+e^-$ -annihilations had been done for massless fermions which was quite sufficient for the purposes of that period [1, 2]. In the meantime the situation has changed in so far as the heavy top quark has been discovered whose production properties in  $e^+e^-$ -annihilations will be studied in the proposed Next-Linear-Collider (NLC). Typical running energies of the NLC would extend from  $t\bar{t}$ -threshold at about 350 GeV to maximal energies of about 550 GeV. It is quite clear that top mass effects cannot be neglected in this energy range even at the highest c.m. energies. It is therefore timely to redo the calculations of [1, 2] for heavy quarks and to investigate the influence of heavy quark mass effects on the polarization observables of the gluon.

As is usual we shall represent the two-by-two differential density matrix  $d\sigma = d\sigma_{\lambda_G \lambda'_G}$  of the gluon with gluon helicities  $\lambda_G = \pm 1$  in terms of its components along the unit matrix and the three Pauli matrices. Accordingly one has

$$d\sigma = \frac{1}{2}(d\sigma \mathbf{1} + d\sigma^x \sigma_x + d\sigma^y \sigma_y + d\sigma^z \sigma_z), \quad (1)$$

where  $d\sigma$  is the unpolarized differential rate and  $d\vec{\sigma} = (d\sigma^x, d\sigma^y, d\sigma^z)$  are the three components of the (unnormalized) differential Stokes vector.

Specifying to  $e^+e^- \rightarrow q(p_1)\bar{q}(p_2)G(p_3)$  we perform an azimuthal and polar averaging over the relative beam-event orientation. After azimuthal averaging the  $y$ -component of the Stokes vector  $d\sigma^y$  drops out [1, 2]. One retains only the  $x$ - and  $z$ -components of the Stokes vector which are referred to as the gluon's linear polarization in the event plane and the circular polarization of the gluon, respectively. The differential unpolarized and polarized rates, differential with regard to the two energy-type variables  $x = 2p_3 \cdot q/q^2$  and  $w = 2(p_1 - p_2) \cdot q/q^2$  (with  $q = p_1 + p_2 + p_3$ ) are then given by

$$\frac{d\sigma^{(x)}}{dx dw} = g_{11} \frac{d\sigma_{U+L}^{1(x)}}{dx dw} + g_{12} \frac{d\sigma_{U+L}^{2(x)}}{dx dw}, \quad (2)$$

$$\frac{d\sigma^z}{dx dw} = g_{14} \frac{d\sigma_{U+L}^{4z}}{dx dw}. \quad (3)$$

The notation  $d\sigma^{(x)}$  stands for either  $d\sigma$  or  $d\sigma^x$ , and the same for  $d\sigma_{U+L}^{i(x)}$  (the index  $i$  is explained later on). This notation closely follows the one in [6] where the nomenclature ( $U + L$ ) has been used to denote the total rate ( $U$ : unpolarized transverse,  $L$ : longitudinal).

The electro-weak cross section is written in modular form in terms of two building blocks. The first building block specifies the electro-weak model dependence through the parameters  $g_{ij}$  ( $i, j = 1, \dots, 4$ ). They are given by

$$\begin{aligned}
g_{11} &= Q_f^2 - 2Q_f v_e v_f \text{Re } \chi_Z + (v_e^2 + a_e^2)(v_f^2 + a_f^2) |\chi_Z|^2, \\
g_{12} &= Q_f^2 - 2Q_f v_e v_f \text{Re } \chi_Z + (v_e^2 + a_e^2)(v_f^2 - a_f^2) |\chi_Z|^2, \\
g_{14} &= 2Q_f v_e a_f \text{Re } \chi_Z - 2(v_e^2 + a_e^2) v_f a_f |\chi_Z|^2, \\
g_{41} &= 2Q_f a_e v_f \text{Re } \chi_Z - 2v_e a_e (v_f^2 + a_f^2) |\chi_Z|^2, \\
g_{42} &= 2Q_f a_e v_f \text{Re } \chi_Z - 2v_e a_e (v_f^2 - a_f^2) |\chi_Z|^2, \\
g_{44} &= -2Q_f a_e a_f \text{Re } \chi_Z + 4v_e a_e v_f a_f |\chi_Z|^2,
\end{aligned} \tag{4}$$

where, in the Standard Model,  $\chi_Z(q^2) = gM_Z^2 q^2 / (q^2 - M_Z^2 + iM_Z \Gamma_Z)^{-1}$ , with  $M_Z$  and  $\Gamma_Z$  the mass and width of the  $Z^0$  and  $g = G_F(8\sqrt{2}\pi\alpha)^{-1} \approx 4.49 \cdot 10^{-5} \text{ GeV}^{-2}$ .  $Q_f$  are the charges of the final state quarks to which the electro-weak currents directly couple;  $v_e$  and  $a_e$ ,  $v_f$  and  $a_f$  are the electro-weak vector and axial vector coupling constants. For example, in the Weinberg-Salam model, one has  $v_e = -1 + 4\sin^2\theta_W$ ,  $a_e = -1$  for leptons,  $v_f = 1 - \frac{8}{3}\sin^2\theta_W$ ,  $a_f = 1$  for up-type quarks ( $Q_f = \frac{2}{3}$ ), and  $v_f = -1 + \frac{4}{3}\sin^2\theta_W$ ,  $a_f = -1$  for down-type quarks ( $Q_f = -\frac{1}{3}$ ). In this paper we use Standard Model couplings with  $\sin^2\theta_W = 0.226$ .

The second building block is determined by the hadron dynamics, i.e. by the current-induced production of a heavy quark pair with subsequent gluon emission. We shall work in terms of the components of the polarized and unpolarized hadronic tensor  $H_{U+L}^{i(x)}$  and  $H_{U+L}^{iz}$  which are related to the differential rates by

$$\frac{d\sigma_{U+L}^{i(x)}}{dx dw} = \frac{\alpha^2}{24\pi q^2} H_{U+L}^{i(x)}, \quad \frac{d\sigma_{U+L}^{iz}}{dx dw} = \frac{\alpha^2}{24\pi q^2} H_{U+L}^{iz}. \tag{5}$$

The index  $i = 1, \dots, 4$  specifies the current composition in terms of the four products of the vector and the axial vector currents according to (we drop all further indices on the hadron tensor)

$$\begin{aligned}
H^1 &= \frac{1}{2}(H^{VV} + H^{AA}), & H^2 &= \frac{1}{2}(H^{VV} - H^{AA}), \\
H^3 &= \frac{i}{2}(H^{VA} - H^{AV}), & H^4 &= \frac{1}{2}(H^{VA} + H^{AV}).
\end{aligned} \tag{6}$$

We mention that, because of parity and charge conjugation parity, the linear combination  $H^3$  does not contribute to the cross section and the spin observables considered in this paper. Eqs. (2) and (3) give the differential cross section for unpolarized beams. The case of longitudinally polarized beams can easily be included and leads to the replacement

$$g_{1i} \rightarrow (1 - h^- h^+) g_{1i} + (h^- - h^+) g_{4i} \quad (i = 1, 2). \tag{7}$$

in the unpolarized and linearly polarized differential rates  $d\sigma_{U+L}^{i(x)}$ . For the circularly polarized rates  $d\sigma_{U+L}^{iz}$  one has the replacements

$$g_{14} \rightarrow (1 - h^- h^+) g_{14} + (h^- - h^+) g_{44} \quad (i = 1, 2). \quad (8)$$

We shall not further discuss beam polarization effects in this letter but refer the interested reader to a more detailed presentation of the subject in [7].

The various pieces of the hadronic tensor can be calculated from the relevant Feynman diagrams and are given by

$$\begin{aligned} H_{U+L}^1(x, w) &= \frac{2\alpha_s N_C C_F q^2}{\pi v} \left[ -2 - 2(4 - \xi)t_+(x, w) \right. \\ &\quad \left. + \left( \frac{(4 - \xi)(2 - \xi)}{x} - 2(4 - \xi) + (4 + \xi)x \right) t_{\ell+}(x, w) \right], \\ H_{U+L}^2(x, w) &= \frac{2\alpha_s N_C C_F q^2 \xi}{\pi v} \left[ -6t_+(x, w) + \left( 3\frac{2 - \xi}{x} - 6 - x \right) t_{\ell+}(x, w) \right], \\ H_{U+L}^{1x}(x, w) &= \frac{2\alpha_s N_C C_F q^2 (4 - \xi)}{\pi v} \left[ -2t_+(x, w) + \left( \frac{2 - \xi}{x} - 2 \right) t_{\ell+}(x, w) \right], \quad (9) \\ H_{U+L}^{2x}(x, w) &= \frac{6\alpha_s N_C C_F q^2 \xi}{\pi v} \left[ -2t_+(x, w) + \left( \frac{2 - \xi}{x} - 2 \right) t_{\ell+}(x, w) \right], \\ H_{U+L}^{4z}(x, w) &= \frac{8\alpha_s N_C C_F q^2}{\pi v} \left[ 2xt_-(x, w) - (2 - x)t_{\ell-}(x, w) \right]. \end{aligned}$$

where  $\xi = 4m_q^2/q^2$ ,  $v = \sqrt{1 - \xi}$ ,  $N_C = 3$ ,  $C_F = 4/3$ , and where we have used the abbreviations

$$t_{\pm}(x, w) := \frac{\xi}{4} \left( \frac{1}{(x - w)^2} \pm \frac{1}{(x + w)^2} \right), \quad t_{\ell\pm}(x, w) := \frac{1}{2} \left( \frac{1}{x - w} \pm \frac{1}{x + w} \right). \quad (10)$$

Note that under quark-antiquark exchange (charge conjugation)  $t_{\pm} \rightarrow \pm t_{\pm}$  and  $t_{\ell\pm} \rightarrow \pm t_{\ell\pm}$ . This implies that the charge conjugation odd contributions  $t_-$  and  $t_{\ell-}$  have a vanishing contribution if one does not discriminate between quarks and antiquarks. In the following we wish to distinguish between the two cases where the quark flavours are identified or where they are not identified. We will refer to these two cases as the flavour tag and flavour no-tag case, respectively.

Let us briefly pause to discuss the mass zero limit of the hadronic tensor components. The mass zero limit can easily be taken by setting  $\xi = 0$  in Eqs. (9). From the terms that remain after taking the  $\xi \rightarrow 0$  limit it is only the terms proportional to  $t_{\ell\pm}(x, w)$  that are important, because they are mass singular as  $\xi \rightarrow 0$ . In fact, when one performs the  $w$ -integration including flavour-tagging, the mass singular

functions  $t_{\ell_{\pm}}(x, w)$  integrate to an  $x$ -independent logarithmic factor  $\ln \xi$  and a finite  $x$ -dependent term  $c_{\pm}(x)$ , i.e.  $\int t_{\ell_{\pm}}(x, w)dw \rightarrow -\ln \xi + c_{\pm}(x)$  (see Eq. (10)). Thus one has

$$\begin{aligned} H_{U+L}^1(x) &\rightarrow -32 \left( \frac{2}{x} - 2 + x \right) \ln \xi, \\ H_{U+L}^{1x}(x) &\rightarrow -32 \left( \frac{2}{x} - 2 \right) \ln \xi, \\ H_{U+L}^{4z}(x) &\rightarrow 32(2 - x) \ln \xi. \end{aligned} \quad (11)$$

The expressions in Eqs. (11) determine the energy dependence of the linear and circular polarization of the gluon in the mass zero limit. They will be used later on when we compare with the corresponding expressions in the massive case.

Returning to the massive quark case we first perform the integration with regard to the phase space variable  $w$ . The integration has to be done between the phase-space boundary curves  $[-w_+(x), w_+(x)]$  where

$$w_+(x) = x \sqrt{\frac{1-x-\xi}{1-x}}. \quad (12)$$

One obtains

$$\begin{aligned} H_{U+L}^1(x) &= \frac{2\alpha_s N_C C_F q^2}{\pi v} \left[ -2 \left( \frac{4-\xi}{x} - (4-\xi) + 2x \right) \frac{1}{x} w_+(x) \right. \\ &\quad \left. + \left( \frac{(4-\xi)(2-\xi)}{x} - 2(4-\xi) + (4+\xi)x \right) t_{\ell_+}(x) \right], \\ H_{U+L}^2(x) &= \frac{2\alpha_s N_C C_F q^2 \xi}{\pi v} \left[ -6 \left( \frac{1}{x} - 1 \right) \frac{1}{x} w_+(x) + \left( 3 \frac{2-\xi}{x} - 6 - x \right) t_{\ell_+}(x) \right], \\ H_{U+L}^{1x}(x) &= \frac{2\alpha_s N_C C_F q^2 (4-\xi)}{\pi v} \left[ -2 \left( \frac{1}{x} - 1 \right) \frac{1}{x} w_+(x) + \left( \frac{2-\xi}{x} - 2 \right) t_{\ell_+}(x) \right], \\ H_{U+L}^{2x}(x) &= \frac{6\alpha_s N_C C_F q^2 \xi}{\pi v} \left[ -2 \left( \frac{1}{x} - 1 \right) \frac{1}{x} w_+(x) + \left( \frac{2-\xi}{x} - 2 \right) t_{\ell_+}(x) \right], \\ H_{U+L}^{4z}(x) &= \frac{8\alpha_s N_C C_F q^2}{\pi v} \left[ 2(1-\xi-x) - (2-x)t_{\ell_-}(x) \right]. \end{aligned} \quad (13)$$

where we have made use of the integrals

$$\begin{aligned} \int_{-w_+(x)}^{+w_+(x)} t_+(x, w) dw &= \left( \frac{1}{x} - 1 \right) \frac{1}{x} w_+(x), \\ \int_{-w_+(x)}^{+w_+(x)} t_{\ell_+}(x, w) dw &= \ln \left( \frac{\sqrt{1-x} + \sqrt{1-x-\xi}}{\sqrt{1-x} - \sqrt{1-x-\xi}} \right) =: t_{\ell_+}(x), \end{aligned} \quad (14)$$

$$\begin{aligned}
2 \int_0^{+w_+(x)} t_-(x, w) &= \frac{1-\xi}{x} - 1, \\
2 \int_0^{+w_+(x)} t_{\ell_-}(x, w) &= \ln\left(\frac{1-x}{\xi}\right) =: t_{\ell_-}(x).
\end{aligned}
\tag{15}$$

It is not difficult to take the  $\xi \rightarrow 0$  limits in Eqs. (12–15) and thereby to reproduce Eq. (11). As was mentioned after Eq. (10), the circular polarization component vanishes in the no-tag case. A non zero result is obtained when the quark flavour is tagged. It is clear that the non-zero result  $H_{U+L}^{Az}$  in Eq. (13) refers to the tag case, i.e., when doing the  $w$ -integration one assumes that the quark and the antiquark can be distinguished. Experimentally, this is not a difficult task for the heavy flavours  $t, b$  and  $c$ .

The normalized linear and circular polarization of the gluon is given by the respective normalized Stokes vector components in Eq. (1). One has

$$P^{x,z}(x) = \frac{d\sigma^{x,z}/dx}{d\sigma/dx}
\tag{16}$$

In Fig. 1(a) we plot the linear polarization of the gluon as a function of the gluon's fractional energy  $x/x_{\max}$  for the top and charm quark cases ( $x_{\max} = 1 - \xi$ ). We use a c.m. energy of 500 GeV. At both ends of the spectrum the linear polarization of the gluon is fixed by general and model independent considerations. At the soft gluon end it is well-known that the linear polarization is 100% while at the hard end of the spectrum the linear polarization has to go to zero for the simple reason that one can no longer define a hadronic plane in this collinear configuration. These limits can be easily verified by taking the corresponding  $x = 0$  and  $x = 1 - \xi$  limits in Eq. (13). We have chosen to compare the polarization of the gluon in the top and charm quark cases at the same fractional energy  $E_G/E_G^{\max} = x/x_{\max}$ . For a given fractional energy  $x/x_{\max}$  the linear polarization of the gluon is always higher in the top quark case than in the charm quark or mass zero case. Contrary to this one finds a higher degree of polarization in the charm quark case than in the top quark case when comparing the linear polarization at *fixed gluon energies*. However, a comparison at a fixed fractional energy of the gluon is more appropriate from a physics point of view in particular if one is interested in the average linear polarization of the gluon to be discussed later on<sup>2</sup>. The linear polarization of the gluon remains above 50% for 85% of the available energy range in the top quark case. As Fig. 1(b) shows, the rate for top quark production is strongly weighted towards smaller gluon energies where the linear polarization is large. We anticipate a large average linear polarization of the

---

<sup>2</sup>In the top mass case and for  $\sqrt{q^2} = 500$  GeV the strength of the leading infrared contribution is given by  $64 \times 0.56/x$  for  $H_{U+L}^1$  and  $48 \times 0.31/x$  for  $H_{U+L}^2$ . This underscores the appropriateness of the fractional energy scale  $x/x_{\max}$  for the comparison since one has the approximate relations  $x/0.56 \cong x/0.31 \cong x/1 - \xi$  with  $1 - \xi = 0.51$

top quark. In the charm quark case the linear gluon polarization is already quite close to the zero mass case which, according to Eq. (11), is given by

$$P^x(x) = \frac{1-x}{1-x+\frac{1}{2}x^2}. \quad (17)$$

The good quality of the zero mass formula Eq. (17) when applied to the charm quark case ( $\sqrt{q^2} = 500 \text{ GeV}$  and  $m_c = 1.3 \text{ GeV}$ ) must be judged against the fact that the dominating logarithmic term  $\log \xi = -10.52$  is not yet overly large.

The linear polarization is flavour independent (and beam polarization independent) in the zero mass limit since the flavour dependent  $g_{11}$  factor drops out in the ratio Eq. (17). This is different in the massive case where flavour dependence comes in through the nonvanishing of the hadron tensor component  $H^2 = \frac{1}{2}(H^{VV} - H^{AA})$ . It can, however, be checked that the dependence on the electro-weak parameters is also quite weak in the massive quark case. The reason is two-fold. First the contributions of  $H^2$  and  $H^{2x}$  are somewhat suppressed even for top quark pair production. Secondly the rate is dominated by one photon exchange at the energy  $\sqrt{q^2} = 500 \text{ GeV}$  leading again to a near cancellation of the electro-weak model dependence.

We have also plotted the circular polarization of the gluon in Fig. 1(a). In the massive quark case the circular polarization is quite small over the whole energy range. Quark mass effects strongly suppress the circular polarization of the gluon as can be seen when one compares with the charm quark case also plotted in Fig. 1(a). Again we found that the circular polarization in the charm quark case is practically identical to the zero mass case given by

$$P^z(x) = -\frac{1}{2} \frac{g_{14}}{g_{11}} \frac{x(2-x)}{1-x+\frac{1}{2}x^2}. \quad (18)$$

The last step is the integration over the second phase-space parameter  $x$ . It is clear that we have to introduce a gluon energy cut-off at the soft end of the gluon spectrum in order to keep the rate finite. Denoting the cut-off energy by  $E_c$  the integration extends from  $x = 2\lambda = 2E_c/\sqrt{q^2}$  to  $x = 1 - \xi$ . We obtain

$$H_{U+L}^1 = \frac{2\alpha_s N_C C_F q^2}{\pi v} \left[ - (4 - \xi) \left[ 2\mathcal{G}(-1) - 2\mathcal{G}(0) - (2 - \xi)\mathcal{G}_\ell(-1) + 2\mathcal{G}_\ell(0) \right] \right. \\ \left. - 4\mathcal{G}(1) + (4 + \xi)\mathcal{G}_\ell(1) \right],$$

$$H_{U+L}^2 = \frac{2\alpha_s N_C C_F q^2 \xi}{\pi v} \left[ - 3 \left[ 2\mathcal{G}(-1) - 2\mathcal{G}(0) - (2 - \xi)\mathcal{G}_\ell(-1) + 2\mathcal{G}_\ell(0) \right] - \mathcal{G}_\ell(1) \right],$$

$$H_{U+L}^{1x} = \frac{-2\alpha_s N_C C_F q^2 (4 - \xi)}{\pi v} \left[ 2\mathcal{G}(-1) - 2\mathcal{G}(0) - (2 - \xi)\mathcal{G}_\ell(-1) + 2\mathcal{G}_\ell(0) \right], \quad (19)$$

$$H_{U+L}^{2x} = \frac{-6\alpha_s N_C C_F q^2 \xi}{\pi v} \left[ 2\mathcal{G}(-1) - 2\mathcal{G}(0) - (2 - \xi)\mathcal{G}_\ell(-1) + 2\mathcal{G}_\ell(0) \right],$$

$$H_{U+L}^{4z} = \frac{6\alpha_s N_C C_F q^2 \xi}{\pi v} \left[ (3 - \xi)(1 - \xi) + 2 \ln \xi \right].$$

where

$$\mathcal{G}(m) := \int_{2\lambda}^{1-\xi} x^{m-1} w_+(x) dx, \quad (20)$$

$$\mathcal{G}(-1) = -\ln\left(\frac{1+v}{1-v}\right) - v \ln\left(\frac{\lambda\xi}{2v^2}\right), \quad (21)$$

$$\mathcal{G}(0) = v - \frac{1}{2}\xi \ln\left(\frac{1+v}{1-v}\right), \quad (22)$$

$$\mathcal{G}(1) = \frac{1}{4}(2 + \xi)v - \frac{\xi}{8}(4 - \xi) \ln\left(\frac{1+v}{1-v}\right), \quad (23)$$

$$\mathcal{G}_\ell(m) := \int_{2\lambda}^{1-\xi} x^m t_{\ell+}(x) dx, \quad (24)$$

$$\begin{aligned} \mathcal{G}_\ell(-1) = & -\frac{1}{2} \ln^2\left(\frac{1+v}{1-v}\right) - \ln\left(\frac{1+v}{1-v}\right) \ln\left(\frac{\lambda\xi}{2v^2}\right) + \\ & + \text{Li}_2\left(\frac{2v}{1+v}\right) + \text{Li}_2\left(\frac{-2v}{1-v}\right) - \text{Li}_2\left(\frac{4v}{(1+v)^2}\right), \end{aligned} \quad (25)$$

$$\mathcal{G}_\ell(0) = -v + \frac{1}{2}(2 - \xi) \ln\left(\frac{1+v}{1-v}\right), \quad (26)$$

$$\mathcal{G}_\ell(1) = -\frac{3}{8}(2 - \xi)v + \frac{1}{16}(8 - 8\xi + 3\xi^2) \ln\left(\frac{1+v}{1-v}\right). \quad (27)$$

In Fig. 2(a) we show a plot of the average linear polarization of the gluon as a function of the c.m. energy  $\sqrt{q^2}$  for three different cut-off values  $E_c = 5, 10$  and  $15 \text{ GeV}$ . Gluon energies of this magnitude are sufficient to make the corresponding gluon jets detectable. The average linear polarization of the gluon rises steeply from threshold and quickly attains very high values around 95% for the top quark case. In the charm quark case the average linear polarization is also large but is somewhat

smaller than in the top quark case. The linear polarization  $P^x$  becomes larger for smaller values of  $\lambda\sqrt{q^2}$  and tends to one as  $\lambda$  goes to zero. The approach to the asymptotic value  $P^x = 1$  is, however, rather low. In Fig. 2(b) we show the average circular polarization of the gluon as a function of the c.m. energy  $\sqrt{q^2}$  for the charm and top cases. In the top quark case the circular polarization of the gluon is quite small as already anticipated from the  $x/x_{\max}$  dependence discussed earlier. The circular polarization in the charm quark case is somewhat larger and reaches values of  $P^z = 3.2\%$  for  $\lambda\sqrt{q^2} = 15 \text{ GeV}$ . The circular polarization  $P^z$  tends to zero as  $\lambda \rightarrow 0$ .

In conclusion we have computed gluon polarization effects in the process  $e^+e^- \rightarrow t\bar{t}G$ . Compared to the zero quark mass case the average linear polarization of the gluon is somewhat enhanced through quark mass effects whereas the circular polarization is considerably reduced through quark mass effects. If one aims to study gluon polarization effects in the splitting process  $e^+e^- \rightarrow t\bar{t}G(\rightarrow GG, q\bar{q})$  the present on-shell calculation should be sufficient to identify and discuss the leading effects of gluon polarization without that one has to perform a full  $O(\alpha_s^2)$  calculation of  $e^+e^- \rightarrow q\bar{q}GG$  and  $e^+e^- \rightarrow t\bar{t}q\bar{q}$  [5].

**Acknowledgements:** This work is partially supported by the BMBF, FRG, under contract No. 06MZ566, and by HUCAM, EU, under contract No. CHRX-CT94-0579. S.G. acknowledges financial support by the DFG, FRG. The work of J.A.L. is supported by the DAAD, FRG.

## References

- [1] H.A. Olsen, P. Osland and I. Øverbø,  
Phys. Lett. **89 B** (1980) 221; Nucl. Phys. **B192** (1981) 33
- [2] J.G. Körner and D.H. Schiller,  
DESY preprint DESY-81-043 (1981), unpublished.
- [3] O.E. Olsen and H.A. Olsen, Phys. Scripta **29** (1984) 12
- [4] S.J. Brodsky, T.A. DeGrand and R. Schwitters, Phys. Lett. **79 B** (1978) 255
- [5] M. Bengtsson and P.M. Zerwas, Phys. Lett. **208 B** (1988) 306
- [6] S. Groote, J.G. Körner and M.M. Tung, “Polar Angle Dependence of the Longitudinal Polarization of Quarks Produced in  $e^+e^-$ -Annihilation”,  
Mainz preprint MZ-TH/95-19, hep-ph/9601313, to be published in Z. Phys. C

- [7] S. Groote, J.G. Körner and J.A. Leyva, “Gluon Polarization in  $e^+e^- \rightarrow t\bar{t}G$ : Polar Angle Dependence and Linear Polarization in the Gluon Beam Plane”, to be published.

## Figure Captions

- Fig. 1: a) Energy dependence of the linear and circular polarization of the gluon. b) Energy dependence of the differential cross section  $e^+e^- \rightarrow t\bar{t}G$  and  $e^+e^- \rightarrow c\bar{c}G$
- Fig. 2: Average linear polarization (a) and average circular polarization (b) of the gluon in  $e^+e^- \rightarrow t\bar{t}G$  and  $e^+e^- \rightarrow c\bar{c}G$  for different values of the cut-off parameter  $\lambda$

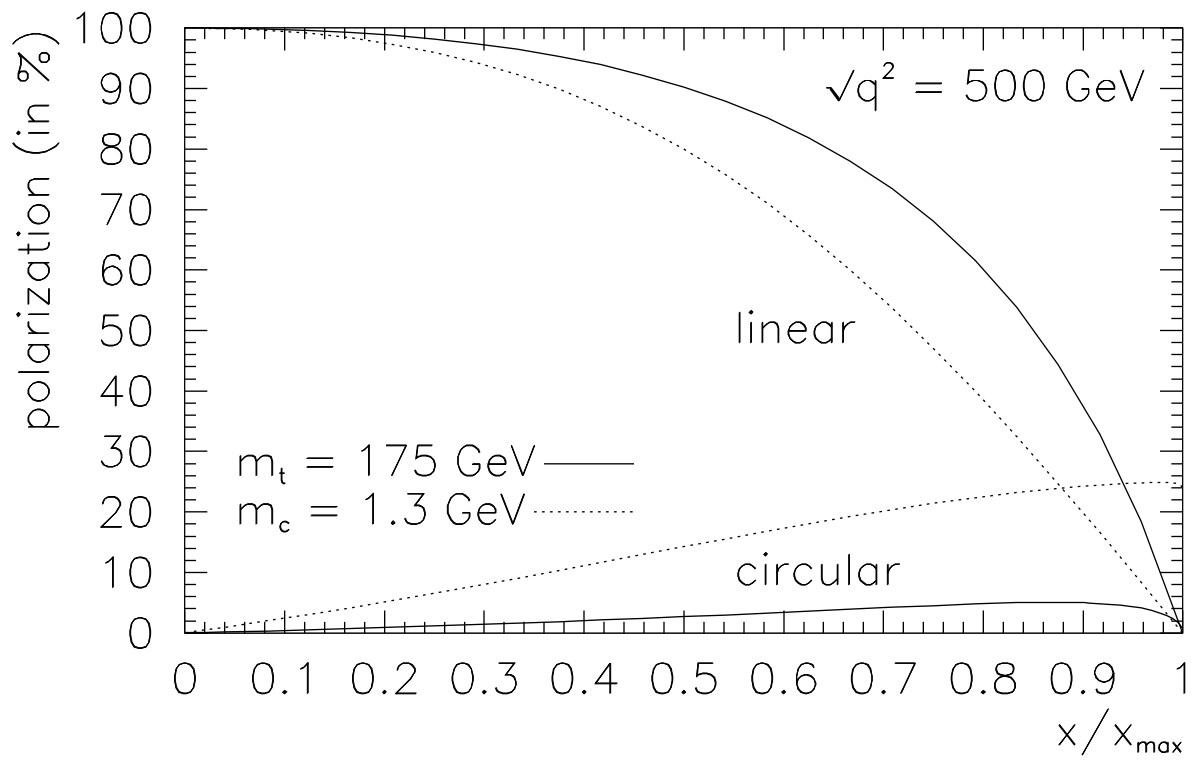


**Figure 1(a)**

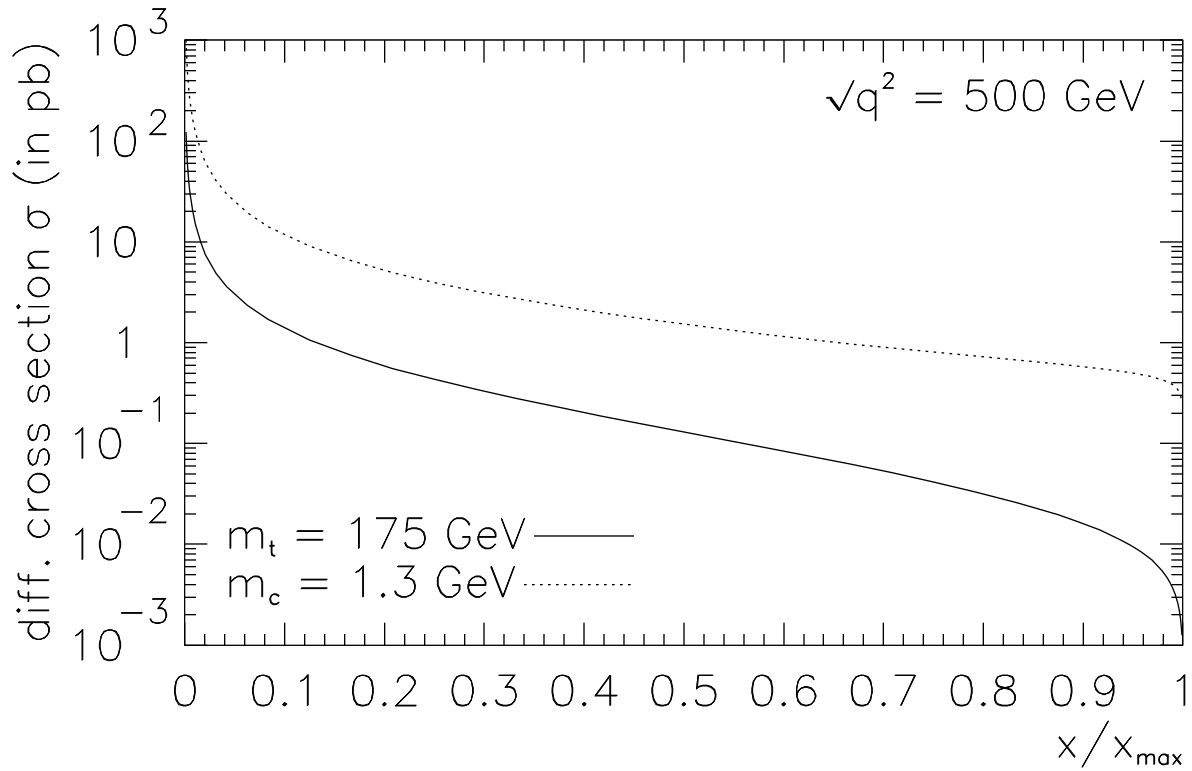


**Figure 1(b)**

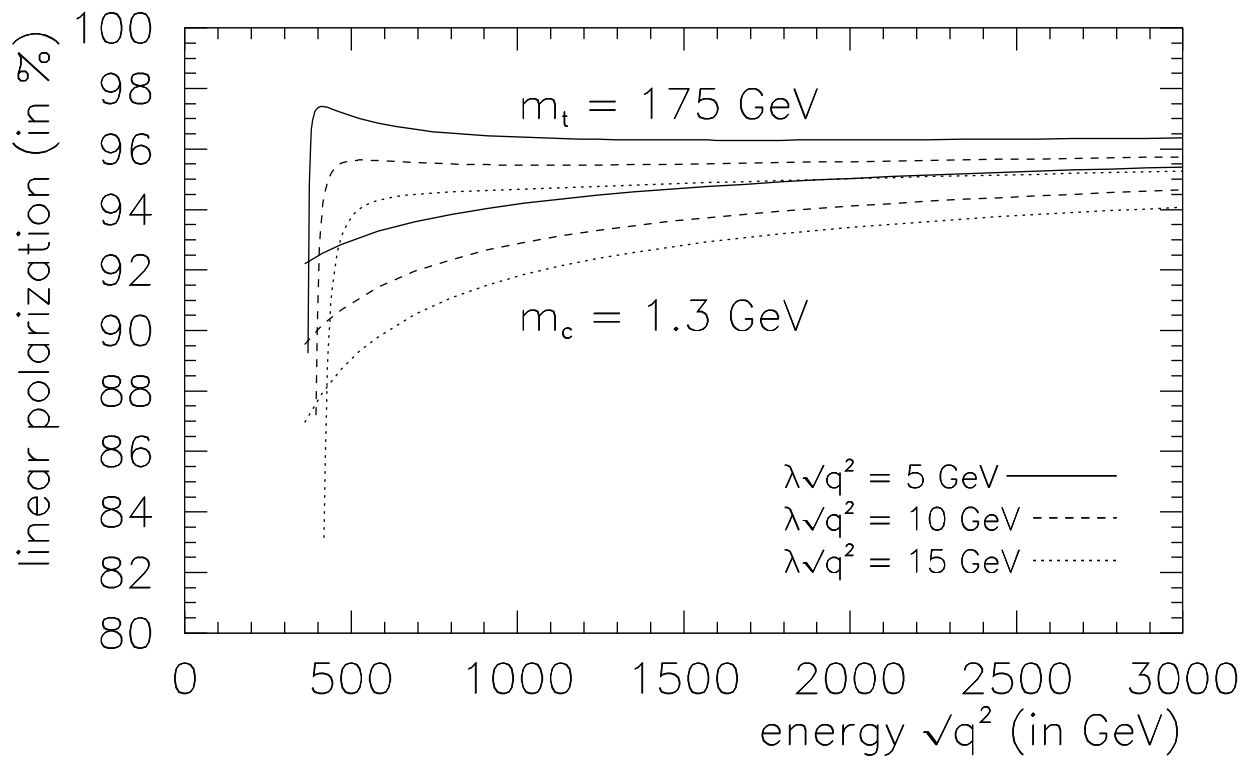


**Figure 2(a)**

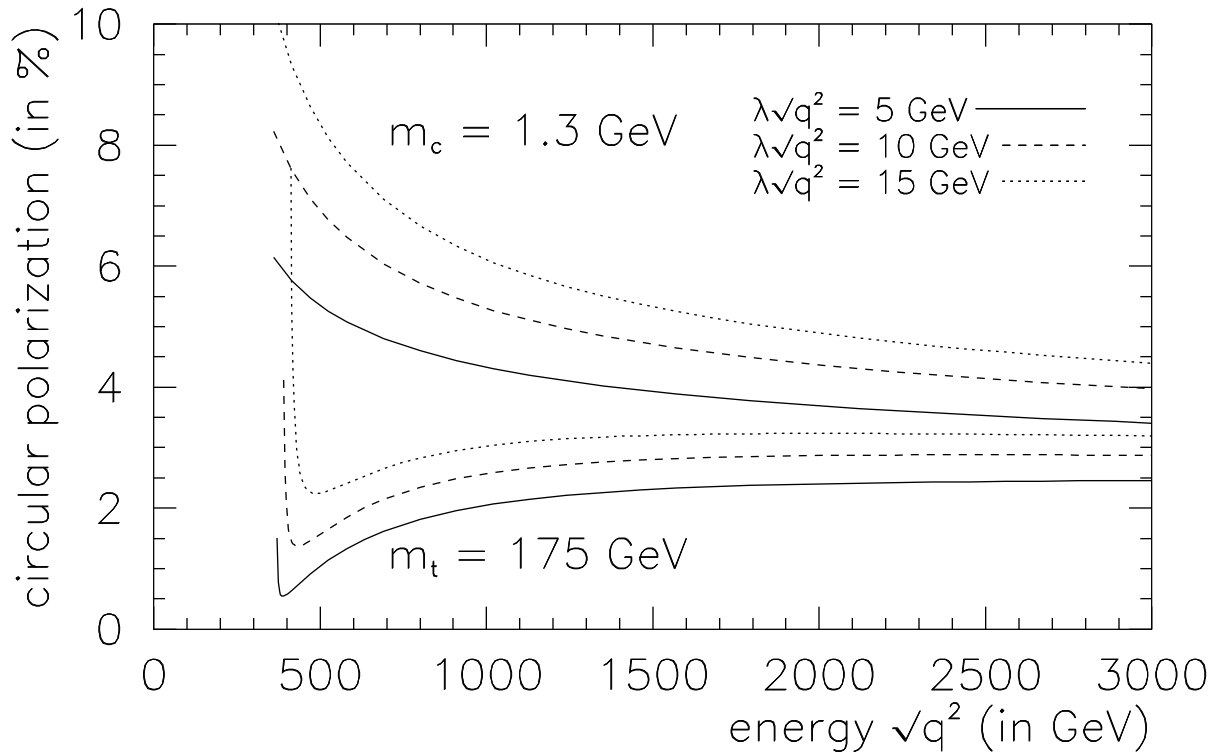


**Figure 2(b)**